Flow Visualization and Measurements in a Two-Dimensional Two-Impinging-Jet Flow

H. Elbanna* and J. A. Sabbagh†
King Abdulaziz University, Jeddah, Saudi Arabia

This paper presents the results of an experimental study of the flowfield characteristics of the interaction of two two-dimensional jets impinging against a normal ground plane. The flowfield was observed visually using oil-flow patterns. Measurements of turbulence and averaged velocities in the flowfield were performed. Parameters included in this investigation were the distance from the ground plane and the jet relative strength. The response of the flowfield to the variation in these parameters has been characterized. Increasing the distance between the jet exit plane and the ground plate, the developed stagnation pressure in the upwash formation region exceeds those corresponding to the jet central streamline. It is found that, in a two-impinging-jet flow, the rate of jet decay is higher than that for a single jet.

Nomenclature

J = velocity momentum $= \int_{\text{exit}}^{\infty} \rho(U^2 + u'^2)\, dy$
J_0 = momentum at nozzle $\text{exit} = t_p \rho(U_{01}^2 + U_{02}^2)$
P = static pressure relative to jet ambient pressure
S = spacing between the centerline of the two nozzles
t_p = jet nozzle width
U = mean velocity in the x direction
u, v, w = fluctuating velocity components along x, y, and z, respectively
$u, 'v, 'w, '$ = rms of fluctuating velocity components along x, y, and z, respectively
x = streamwise coordinate along centerline
y = coordinate normal to the centerline
z = coordinate normal to the confining walls
ρ = density

Subscripts
01 = exit plane conditions of the strong jet
02 = exit plane conditions of the weaker jet

Introduction

THE impingement of two parallel ventilated jets on a normal plane surface (Fig. 1) is of interest in many engineering problems, particularly in the design of efficient VTOL aircraft. Ingestion of exhaust gases increase the temperature at engine inlet, leading to significant reduction in performance. It may even cause stalling of the engine in the case of very high temperature rise and/or large fluctuations in temperature.[1] The flowfield due to in-ground effects (IGE) is classified into two types: near-field and far-field flows. Far-field flows are encountered when the jets are placed close enough or when the jets are sufficiently far from the ground. In this situation, the two jets combine prior to striking the ground, and the confluent jet spreads as a wall jet. Because of entrainment of air by the exhausting jets and buoyancy effects, some of the warmer gases in the decayed wall jet may be brought into the engine inlets. Far-field ingestion is low because hot gases drawn back to the engine inlets are subjected to a long path and extensive mixing, and thus they reach the inlets at temperatures close to the ambient. Near-field ingestion occurs when the two jets are placed far enough apart. In this case, the flowfield of each of the two impinging jets exhibits the normal behavior of a wall jet. In addition, the interior wall jets meet, forming an upward flow called upwash or "fountain." In near-field ingestion, exhaust gases in the fountain have a shorter path to the inlets, and accordingly high temperature levels are usually associated with it.

Enhanced entrainment of ambient air creates subatmospheric pressures on the undersides of the aircraft, resulting in a downward force (lift loss). This negative force, which is termed "suckdown," results in an effective vertical thrust loss. However, capturing some of the upwash flow produces positive lift force resulting from increased pressure on the undersurface of the aircraft. Favorable effects of the fountain compensate for and may even exceed suckdown losses.

The most elementary flowfield appropriate to this discussion is that of free parallel jets. Such a flowfield has been subject to extensive investigation by the authors[2-5] and other workers.[6-11] Air entrained by the two jets causes a subatmospheric region to exist between the two nozzles. There would be an attraction between the two jets, causing their axes to curve and eventually merge, forming a single jet. It was concluded also[2] that "ventilated" (free-standing) jets are confluent at larger distance from nozzle exit than that for "unventilated" jets.

Aerodynamic suckdown effects in ground proximity was investigated[12] for a full-scale configuration and compared with results from small-scale tests. It was concluded that valid aerodynamic suckdown data applicable to a full-scale configuration can be obtained from small-scale tests. Upwash from full-scale, heated, compressible aircraft engine jets has been accurately predicted from small-scale cold-jet incompressible experiments.[13]

Available work found in the literature is concerned with impingement of round jets.[14-19] In most of these investigations, measurements were conducted using Kiel, total, and static pressure probes and were mainly devoted to measuring the induced forces and moments. In the reviewed previous work, a maximum value of H/d of 10 was investigated in the work of Ref. 20, and a maximum value of S/d of 12 is found in the work of Ref. 21. Within these limits of flow parameters, it was concluded[17,18] that velocity fluctuations were high enough and scale of turbulence was large enough to bring about a significant error in the measured flow parameters. Rectangular

Received May 27, 1987; revision received March 11, 1988.

*Assistant Professor, Department of Thermal Engineering. Member AIAA.
†Professor, Department of Thermal Engineering.

nozzles with the longer sides parallel were found to reduce suckdown effect rather than round jets.[22] In spite of the considerable efforts expended in studying the problem for many years, extensive measurements of mean velocities and the turbulent structure of the flowfield have not been carried out and thoroughly studied. Detailed measurements are also needed in order to develop accurate prediction methods.

The results presented in the next sections are concerned with the impingement of two two-dimensional jets on a plane normal to their axes. The jets are placed far enough apart to minimize the interaction between the upwash and the jet plumes. Parameters included in this investigation are the distance between the jet exit plane and the ground plane, and relative jet strength.

The effects of these parameters were studied by visually observing the flowfield using oil-flow patterns and silk tuft probes. Ground-pressure measurements were obtained using pressure taps. Lateral traverses of mean velocity and turbulent intensitites were carried out using a DISA 5600 two-channel, hot-wire anemometer. The objective of the experimental results is to study the influence of the preceding parameters on the upwash and other flow properties. A second objective of this work is to investigate the turbulence structure of the flowfield. This serves to develop more accurate models to predict upwash and suckdown effects on VTOL aircraft.

Apparatus and Procedure

Air is supplied from two separate blowers to two identical nozzle blocks (Fig. 2). Before it converges to the nozzle exit, air passes through three grids for producing uniform velocity along the length of the slot. The contraction ratio is 13:1, and the nozzle slot has a width $t_p = 5.5$ mm and a length $l = 490$ mm. The two nozzle blocks are confined between two parallel walls. The apparatus is designed such that the nozzle slot spans all of the distance between the two confining walls to prevent air leak into the low-pressure regions between the two jets. In the impinging jet experiments, a ground plate is placed vertically between the two horizontal confining walls normal to the nozzle axes. The confining walls extend 1 m to either side of the midline between the two jets.

Traverses were carried out spanwise of the nozzle slot and in the lateral direction to determine the degree of uniformity of the flow emanating from the nozzle. Spanwise velocity traverses have shown that, over the middle of 80% of the distance between the lower and upper walls, the velocity is highly uniform. Lateral traverses revealed a very flat velocity profile. The present nozzle design, with a contraction ratio of 13.1 and aspect ratio of 89.1, is considered good for the two-dimensionality of the flowfield. However, several traverses were carried out at different levels in the central 80% of the distance between the bottom and upper confining walls. These measurements have shown that the flowfield exhibits good two-dimensionality.[23]

The characteristics of the single jet used in the present experiments were studied[23] and compared with available work in the literature.[24-26] The ratio of the momentum at downstream stations to that at the nozzle exit plane J/J_0 was found to be 0.93. This relatively high value of J/J_0 indicates that the nozzles are well designed.

In the present experiments, the spacing between the two nozzles is fixed at 27.6 slot widths t_p. Such a high value of S/t_p has the advantage of reducing the interaction between jet plumes and the upwash. The velocity of the strong jet U_{01} was kept constant at 54.5 m/s, corresponding to a Reynolds number of 16,600 based on the slot width t_p. The velocity of the second jet U_{02} was changed by obstructing the blower inlet. Velocity ratios were varied over a range from 1 to 0.5. Within this velocity range, the characteristics of the two parallel freejets were also studied, and the principle of conservation of momentum was satisfied.[2,23]

Another parameter in this investigation is the distance H between the nozzle exit plane and the ground plane. The H/t_p values investigated are 14.7, 30, 40, and 50. In most of the previous work in the literature, the ground plane was placed at a distance not greater than the core of the incident jets. In this case, the wall jet flow is influenced by the high turbulence level in the outer shear layer of the flow developing region. Also, upwash measurements become close to the origin of the upwash. This leads to a high turbulence level in the upwash region, as was previously noticed[17,18] for low values of H/t_p.

Mean velocities and turbulent quantities were measured using a DISA 5600 hot-wire anemometer. Most measurements were conducted using X-probes 55P63 and 55P64 manufactured by DISA. For these probes, the wire diameter is 5μ, and its active length is 1.2 mm. The distance between the two axes of the X-wire probe is of the order of one wire length. For such a distance, it was concluded[27] that the thermal wake effects are avoided and that the wire can be considered to have no pitch sensitivity. The X-wire probe can be used in oblique operation for measurements of mean velocities and turbulent intensities with adequate accuracy[28,29] up to an angle of 25 deg. For Reynolds shear stress, higher errors are obtained with oblique operation.

A silk tuft probe was mutually traversed with the hot-wire probe. The two probes were arranged to be located in the same measuring position but at a small distance apart in the Z direction. The flow direction was obtained by observing the tuft direction together with photographs of oil-flow patterns, which were obtained by spreading a mixture of kerosene and chalk on a perspex sheet placed horizontally between the jet exit plane and the ground plane.

Surface pressure distributions along the ground plate were measured from pressure taps of 0.5 mm diam. Pressure taps were evenly distributed in the middle part of the ground plate. Connecting the pressure taps to a tilting manometer, large

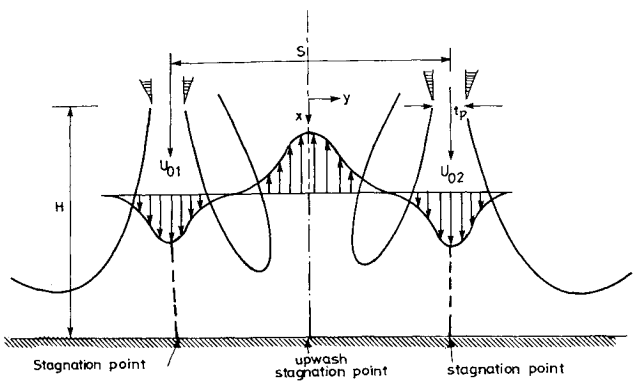

Fig. 1 Two-jet impingement model.

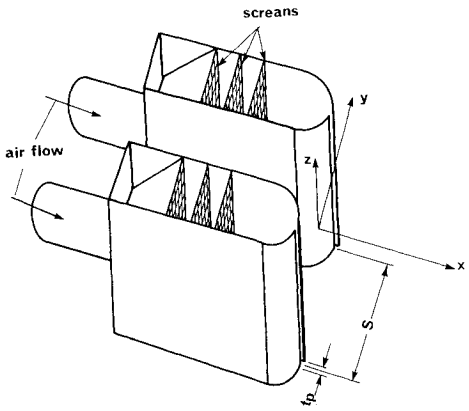

Fig. 2 The nozzle blocks.

fluctuations in pressure were noticed. Therefore, pressure measurements were displayed using a pressure transducer and electronic manometer. Average pressure values were obtained by connecting the analog output of the electronic manometer to a DISA 55D35 voltmeter.

Results and Discussion

Flow Visualization

Flow visualization technique is an interesting tool that provides valuable insight into complex flowfields. Figure 3 shows the flow pattern for the impingement of two jets of equal strength. Figures 3a–3d describe how the nature of the flowfield is influenced by changing the distance H between the nozzle exit plane and the ground plate. Two outside free wall jets arising from the impingement of the two jets on the ground plane are clearly seen. The upwash formed by collision of the interior opposed wall jets is clearly observed midway between the two jets. Entrainment effects caused by the downstream moving jets and upstream moving fountain lead to the formation of two counter-rotating vortices that are clearly seen between the two jets and the fountain. Increasing H/t_p, the jet spreads further before striking the ground plate. Accordingly, the jet impingement region increases. In Figs. 3c and 3d a stagnation region is observed as the upwash approaches the nozzle exit plane. In these figures, part of the upwash flow is doubled back into the vortices, whereas the remaining upwash flow eventually meets the downward entrained flow between the two jets, and a stagnation region is found. The stagnation region is more noticeable at $H/t_p = 50$ because the upwash is subjected to a large path and consequently to more deceleration. An interesting feature is the location of the vortices' center. Although it seems to be midway between the nozzle exit plane and the ground plane for $H/t_p = 30$, it comes closer to the jet exit plane for $H/t_p = 40$ and 50. In Fig. 3b, it seems that the upwash and the counter-rotating vortices are pushing the jet plumes in the outward direction.

Figures 4a–4d show the effect of changing the velocity ratio of the two jets U_{02}/U_{01} on the impingement flowfield. In Figs. 4a–4b, it can be seen that the upwash curves toward the strong jets as the jets have different strength. For smaller values of H/t_p, previous investigators (e.g., Refs. 17 and 21) had shown that the upwash deflects toward the weaker jet as the velocity ratio decreases. However, this finding is also observed in the present work for $H/t_p = 30$ and $U_{02}/U_{01} = 0.5$ (Fig. 5b). As may be seen in Figs. 4a–4d, as the velocity ratio decreases, the area of the right vortex (in the weaker jet side) increases, whereas the left vortex becomes narrower in the lateral direction, and its effect extends deeper toward the ground plate. In all visualized flows with different jet strengths, it can be seen that the strong jet slides under the weaker jet on the right. As a result, the right wall jet is much thicker than the left one. This feature is more evident as the velocity ratio decreases. In Fig. 5a for $H/t_p = 14.7$ and $U_{02}/U_{01} = 0.5$, it seems that the left vortex has disappeared and the flow comprising it has drawn into the weaker jet side. It can be detected also that the flow direction of the right vortex is anticlockwise, opposite to what was observed for the equal-strength jets. Of significant interest in this figure is that the upwash has disappeared and the flow between the two jets is in the downstream direction.

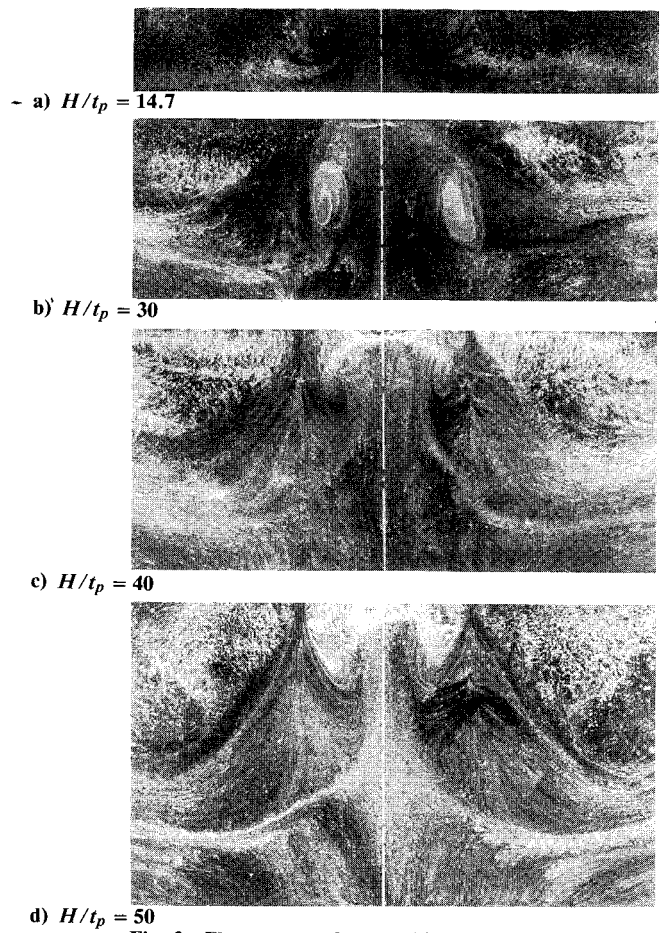

a) $H/t_p = 14.7$

b) $H/t_p = 30$

c) $H/t_p = 40$

d) $H/t_p = 50$

Fig. 3 Flow pattern for equal impinging jets.

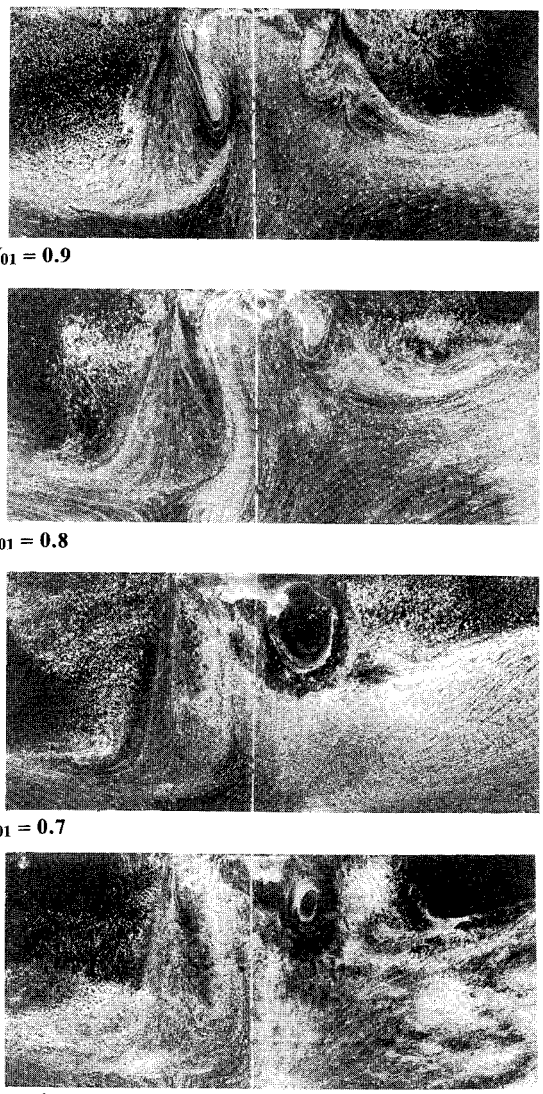

a) $U_{02}/U_{01} = 0.9$

b) $U_{02}/U_{01} = 0.8$

c) $U_{02}/U_{01} = 0.7$

d) $U_{02}/U_{01} = 0.6$

Fig. 4 Flow pattern for unequal impinging jets: $H/t_p = 40$.

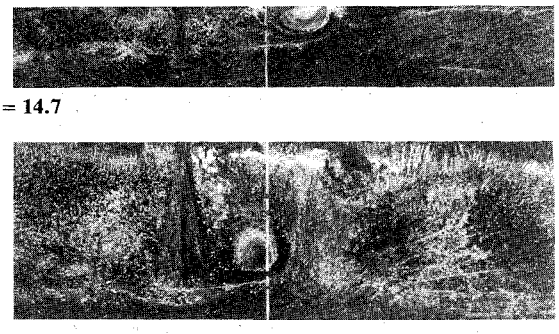

a) $H/t_p = 14.7$

b) $H/t_p = 30$

Fig. 5 Effect of varying the height H/t_p on the flow pattern at a velocity ratio $U_{02}/U_{01} = 0.5$.

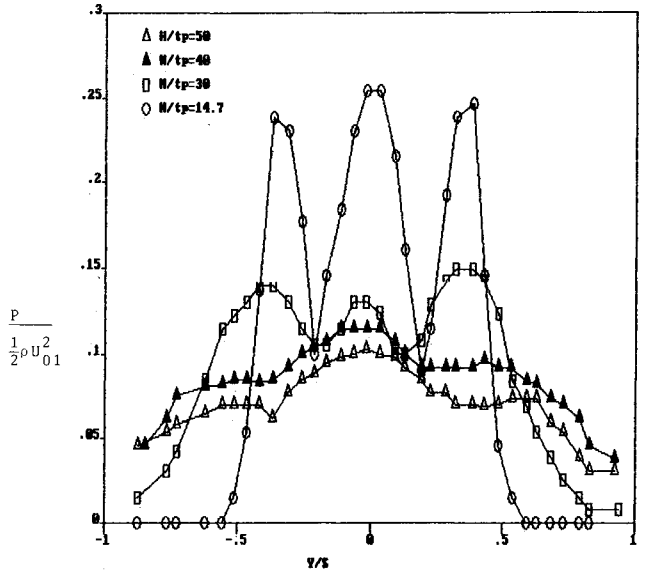

Fig. 6 The distribution of ground pressure for equal impinging jets: $H/t_p = 14.7$.

Ground-Pressure Measurements

The variation of ground pressure for equal-strength jets is shown in Fig. 6 for different values of H/t_p. As the two incident jets approach the impinging region, the velocity in the jet decays with a rate much greater than that for a freejet, and consequently the pressure increases above the ambient surrounding pressure. Along the ground plate, two peak pressure values are found, corresponding to the impingement of the two jets. Midway between the two impinging regions, a stagnation pressure is developed where the flow comes to rest and deflects upstream, forming the upwash. For $H/t_p = 14.7$, the upwash centerline stagnation pressure compares with the peak pressure values corresponding to the two jets, whereas it exceeds those of the nozzles at H/t_p values of 40 and 50. This observation contradicts the conclusions of Refs. 19 and 30 that the upwash stagnation pressure will never achieve the nozzle impinegment peak pressure value, whatever the spacing between the two nozzles or their relative distance from the ground plate. In the interior wall jet region, the pressure is greater than ambient. This shows that, for the investigated values of H/t_p, the spacing between the two nozzles is not enough for the interior wall jets to be completely developed, and therefore pressure recovery does not occur prior to interaction.

When the two jets have different strengths, the distribution of ground pressure becomes asymmetrical. Figure 7 shows the

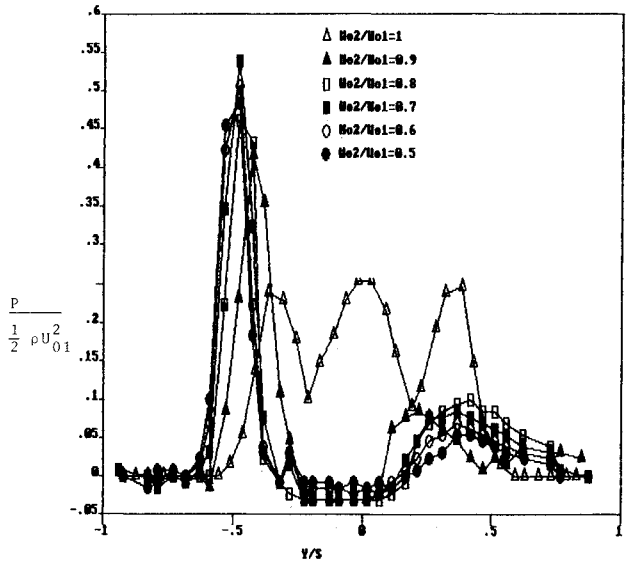

Fig. 7 The distribution of ground pressure for unequal impinging jets: $H/t_p = 14.7$.

ground-pressure distribution for $H/t_p = 14.7$ and for U_{02}/U_{01} values ranging from 0.5 to 0.9. A dramatic change occurs in the pressure distribution, even for $U_{02}/U_{01} = 0.9$. Negative pressure is found on the ground plane in the region between the two jets. The development of pressure lower than ambient in this region is attributed to air entrainment into the wall jet. As the velocity ratio decreases, it can be seen the the peak pressure corresponding to the strong jet increases. At $U_{02}/U_{01} = 0.7$, it attains a maximum value of about twice that obtained with equal-strength jets. Then it decreases slightly with a further decrease in the velocity ratio. Therefore, the pressure in the impingement region of jet is highly influenced by the existence of the second jet. This shows that we cannot predict pressure data in the impingement region from single-impingement jet data, as was usually considered by previous workers.[19,30,31] Such treatment would be subjected to considerable error, especially at higher values of H/t_p. From Fig. 7, it can be noticed that the location of the peak pressure corresponding to the strong jet is also influenced by the velocity ratio. It moves away from the midline between the two nozzles and approaches the nozzle centerline as the velocity ratio decreases. This is due to the lesser attraction of the two jets at lowered velocity ratio.

Hot-Wire Measurements

Figures 8–11 show the results of hot-wire lateral traverses for the two equal impinging jets with the ground plate at a distance $H/t_p = 14.7$. Lateral traverses were conducted upstream and downstream of the nozzle exit plane from $x/t_p = -3$ up to $x/t_p = 8$. Mean velocity data are presented in Fig. 8. From lateral velocity traverses, the velocity along the jet central streamline is detected. Consequently, the extension of the potential core and the rate of jet decay are obtained. The jet potential core region is shortened to less than three nozzle slot widths t_p. The jet velocity decays in a faster rate than that for a single jet and free parallel jets. In the interjet passage close to the outer shear layer of each of the two jets, entrained flow is quite noticeable. Near the nozzle exit plane at $x/t_p = 1$, the velocity of the entrained secondary flow is in the order of 0.35 U_{01}. The reversed upwash flow is clearly observed between the two jets. Flow direction in this region was obtained by a tuft that was mutually traversed with the hot-wire probe. Because the flow is two-dimensional, it was possible to place the tuft probe in the same flowfield position as the hot-wire probe. The interaction of the downstream entrained flow and the up-

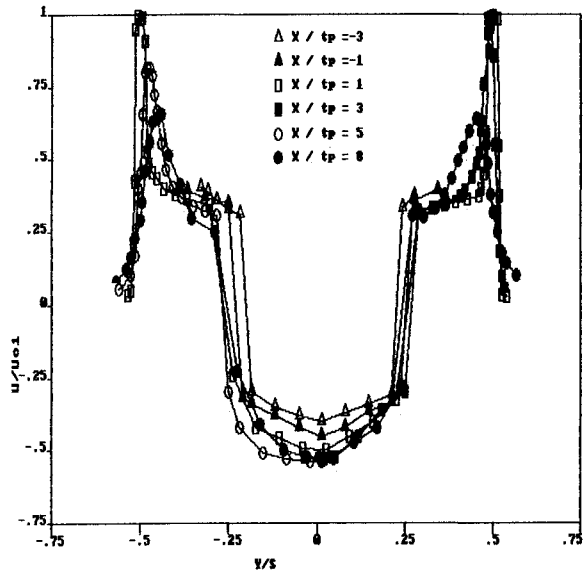

Fig. 8 Velocity distribution: $H/t_p = 14.7$, $U_{02}/U_{01} = 1$.

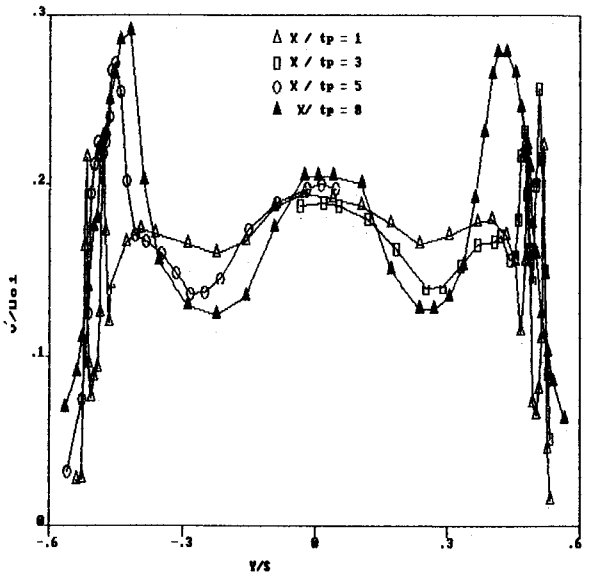

Fig. 10 Lateral turbulence intensity: $H/t_p = 14.7$, $U_{02}/U_{01} = 1$.

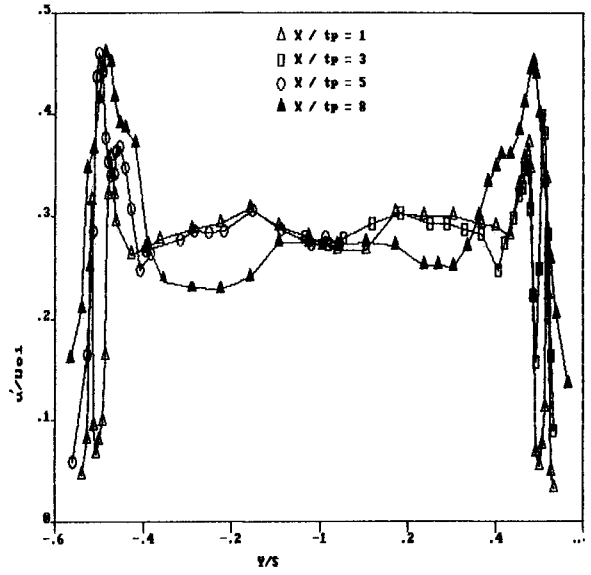

Fig. 9 Longitudinal turbulence intensity: $H/t_p = 14.7$, $U_{02}/U_{01} = 1$.

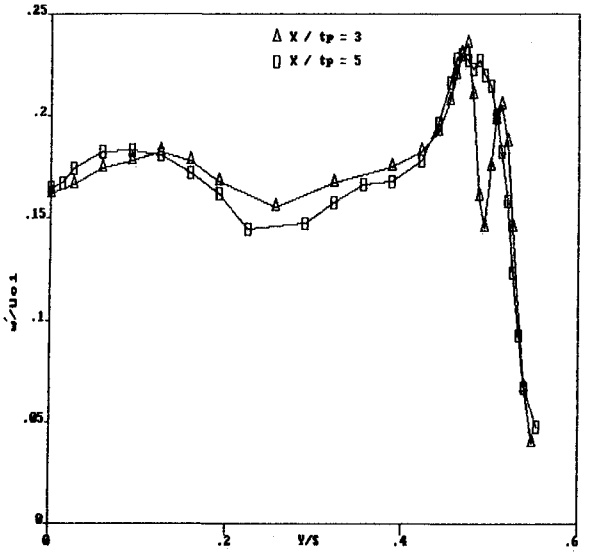

Fig. 11 Transversal turbulence intensity: $X/t_p = 14.7$, $U_{02}/U_{01} = 1$.

stream moving fountain creates two counter-rotating vortices. In regions at the edge of the upwash and the shear layers of the incident jets, the flow direction was highly fluctuating, and complete velocity reversal was observed to occur quite frequently. Hot-wire measurements were not tried in these regions. The colliding two interior wall jets generate high pressure in the upwash formation region. This high pressure is transformed into kinetic energy, and the upwash is accelerated rapidly to a maximum value upstream of the ground plate. The velocity in the upwash decays with further distance from the ground plate due to spreading and enhanced entrainment. At the nozzle exit plane, the upwash centerline velocity is about 0.5 U_{01}.

The distribution of the turbulent intensities u', v', and w' are shown in Figs. 9–11, respectively. At the nozzle incidence region close to the nozzle exit plane, peak values correspond to the nozzle edges, whereas minimum values are related to the jet core. In regions of high turbulent intensity, the flow is essentially in the downstream direction. In other investigated regions where the turbulence intensity is relatively low, the inclination of the mean flow to the downstream direction is not

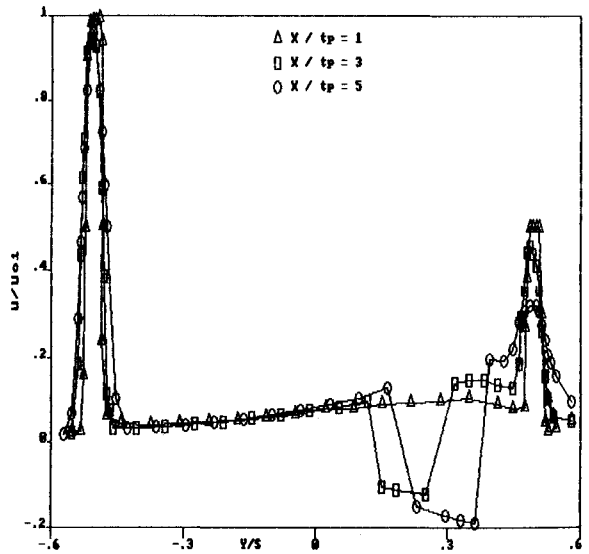

Fig. 12 Velocity distribution: $H/t_p = 14.7$, $U_{02}/U_{01} = 0.5$.

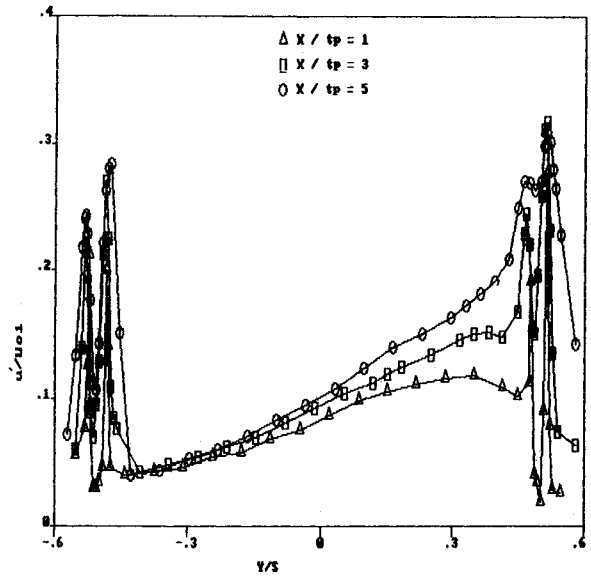

Fig. 13 Longitudinal turbulence intensity: $H/t_p = 14.7$, $U_{02}/U_{01} = 0.5$.

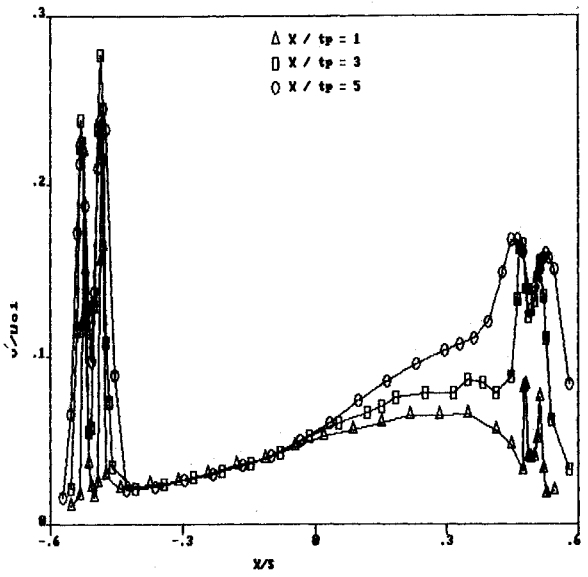

Fig. 14 Lateral turbulence intensity: $H/t_p = 14.7$, $U_{02}/U_{01} = 0.5$.

greater than 30 deg. Guided by the work of Klatt[28] and Champange and Sleicher,[32] the maximum errors in the measured values of u'/U_{01}, v'/U_{01}, and w'/U_{01} are estimated[23] to be about 5.5%, 19%, and 19%, respectively. The turbulent structure in the upstream region shows a great departure from isotropy.

The velocity profile for impinging jets with unequal strength is shown in Fig. 12 for $U_{02}/U_{01} = 0.5$ and $H/t_p = 14.7$. It can be seen that the weaker jet decays and spreads at a rate much greater than the strong jet. At $x/t_p = 3$ and 5, reversed flow is found in a narrow region closer to the weaker jet. The reversed flow disappears at $x/t_p = 1$. Comparison of Figs. 8 and 12 shows that the characteristics of the flowfield are greatly influenced by the velocity ratio of the two jets. At the nozzle exit plane, the strong upwash has disappeared for $U_{02}/U_{01} = 0.5$. In the region between the two jets, Figs. 13 and 14 show higher turbulent intensities near the weaker jet side. These higher intensities are related to the reversed flow observed in this region. However, turbulent intensities in this case are much lower than those in the upwash region for equal-strength jets.

Conclusions

In this paper, measurements of mean velocities, pressure, and turbulent intensities together with flow visualization experiments were conducted to study the flowfield of two jets impinging normal to a ground plate. Flow visualization studies have shown the influence of both geometric parameters and the relative strength of the two jets on the fountain as well as other flow properties. When the ground plate is placed far from the nozzle exit plane at $H/t_p = 40$, it is found that the upwash deflects toward the strong jet as the velocity ratio of the two jets decreases.

Ground-pressure measurements have shown that, as H/t_p increases, stagnation pressure in the upwash formation region exceeds that in the impinging region of the two jets. When the impinging jets have unequal strength, the strong jet slides under the weaker jet, and ground-pressure measurements show negative values in the upwash formation region.

Hot-wire measurements have shown that the rate of jet decay in a two-impinging-jet flow is greater than that for a freejet and for a single impinging jet. For asymmetric impingement conditions developed by unequal-strength jets, the weaker jet spreads and decays at a rate much greater than that of the strong jet.

Acknowledgment

This work was funded by the College of Engineering, King Abdulaziz University, Grant No. 05-413.

References

[1]Kuhn, R. E., "Design Concepts for Minimizing Hot-Gas Ingestion in V/STOL Aircraft," *Journal of Aircraft*, Vol. 19, Oct. 1982, pp. 845-850.

[2]Elbanna, H. and Sabbagh, J. A., "Interaction of Two Nonequal Plane Parallel Jets," *AIAA Journal*, Vol. 25, Jan. 1987, pp. 12-13.

[3]Elbanna, H., Gahin, S., and Rashed, M. I. I., "Investigation of Two Plane Parallel Jets," *AIAA Journal*, Vol. 21, July 1983, pp. 986-991.

[4]Elbanna, H., Sabbagh, J. A., and Rashed, M. I. I., "Interception of Two Equal Turbulent Jets," *AIAA Journal*, Vol. 23, July 1985, pp. 985-986.

[5]Elbanna, H. and Sabbagh, J. A., "Interaction of Two Nonequal Jets," *AIAA Journal*, Vol. 24, April 1986, pp. 686-687.

[6]Marsters, G. F., "Interaction of Two Plane, Parallel Jets," *AIAA Journal*, Vol. 14, Dec. 1977, pp. 1756-1762.

[7]Tanaka, E., "The Interference of Two-Dimensional Parallel Jets (1st Rept.)," *Bulletin of the JSME*, Vol. 13, No. 56, Feb. 1970, pp. 272-280.

[8]Tanaka, E., "The Interference of Two-Dimensional Parallel Jets (2nd Rept.)," *Bulletin of the JSME*, Vol. 17, No. 109, July 1974, pp. 920-927.

[9]Miller, D. R. and Comings, E. W., "Force-Momentum Fields in a Dual-Jet Flow," *Journal of Fluid Mechanics*, Vol. 17, Feb. 1960, pp. 237-256.

[10]Murai, K., Taga, M., and Akagaw, K., "An Experimental Study on Confluence of Two Two-Dimensional Jets," *Bulletin of the JSME*, Vol. 19, No. 134, Aug. 1976, pp. 958-964.

[11]Shimoda, S. Y. F. and Jotaki, T., "Hot Wire Measurements in the Interacting Two-Plane Parallel Jets," *AIChE Journal*, Vol. 25, No. 4, July 1979, pp. 676-678.

[12]Hall, G. R., "Scaling of VTOL Aerodynamic Suckdown Forces," *Journal of Aircraft*, Vol. 4, April 1967, pp. 293-304.

[13]Hill, W., Jr., Jenkins, R. C., and Dudley, M. R., "An Investigation of Scale Model Testing of VTOL Aircraft in Hover," International Congress of the Aeronautical Sciences, Paper 82-5.2.2, Aug. 1982.

[14]Adakar, D. B. and Hall, G. R., "The Fountain Effect and VTOL Exhaust Ingestion," AIAA Paper 68-79, 1968.

[15]Houlihan, T. M. and Thompson, C. D., "Jet Impingement under VTOL Aircraft," *AIAA Journal*, Vol. 10, Sept. 1972, pp. 1179-1182.

[16]Hill, W. G., Jr. and Jenkins, R. C., "Experimental Investigation of Multiple Jet Impingement Flows Applicable to VTOL Aircraft in

Ground Effect," Grumman Research Dept., Memo. RM-605, Nov. 1975.

[17]Jenkins, R. C. and Hill, W. G., Jr., "Investigation of VTOL Upwash Flows Formed by Two Impinging Jets," Grumman Research Dept., Rept. RE-548, Nov. 1977.

[18]Lummus, J. R., "The Criticality of Engine Exhaust Simulations on VSTOL Model-Measured Ground Effects," Office of Naval Research, Rept. ONR-CR212-255-IF, Aug. 1979.

[19]Hill, W. G., Jr. and Jenkins, R. C., "Effect of Nozzle Spacing on Ground Interference Forces for a Two-Jet V/STOL Aircraft," *Journal of Aircraft*, Vol. 17, Sept. 1980, pp. 684-689.

[20]Mclemore, H. C. and Smith, C. C., Jr., "Hot-Gas Ingestion Investigation of Large-Scale Jet VTOL Fighter-Type Models," NASA TN D-4609, 1969.

[21]Saripalli, K. R., "Visualization of Multi-Jet Impingement Flow," AIAA Paper 81-1364, July 1981.

[22]Louisse, J. and Marshall, F. L., "Prediction of Ground Effects for VTOL Aircraft with Twin Lifting Jets," *Journal of Aircraft*, Vol. 13, Feb. 1976, pp. 123-127.

[23]Sabbagh, J. A. and Elbanna, H., "Investigation of Two Impinging Jets as Applied to VTOL Aircraft," College of Engineering, King Abdulaziz Univ., Saudi Arabia, Progress Rept. 05-413, March 1987.

[24]Heskestad, G., "Hot Wire Measurement in a Plane Tubulent Jet," *Transactions of ASME, Journal of Applied Mechanics*, Vol. 32, Dec. 1965, pp. 721-734.

[25]Bradbury, L. J. S., "The Structure of a Self-Preserving Turbulent Plane Jet," *Journal of Fluid Mechanics*, Vol. 23, Pt. 1, 1965, pp. 31-64.

[26]Gutmark, E. and Wygnaski, J., "The Plannar Turbulent Jet," *Journal of Fluid Mechanics*, Vol. 73, Pt. 3, 1976, pp. 465-495.

[27]Jerome, F. E., Gutton, D. E., and Patel, R. P., "Experimental Study of the Thermal Wake Interference Between Closely Spaced Wires of a X-type Hot-Wire Probe," *Aeronautical Quarterly*, Vol. 23, May 1971, pp. 119-126.

[28]Klatt, F., "The X Hot-Wire Probe in a Plane Flow Field," *DISA Information*, No. 8, July 1969, pp. 3-11.

[29]Bruun, H. H., "Interpretation of X Hot-Wire Signals," *DISA Information*, No. 18, Sept. 1975, pp. 5-10.

[30]Siclari, M. J., Hill, W. G., Jr., Jenkins, R. C., and Migdal, D., "VTOL IN-Ground Effect Flows for Closely Spaced Jets," AIAA Paper 80-1980, Aug. 1980.

[31]Hill, W. G., Jr., "Effects of a Central Fence on Upwash Flows," *Journal of Aircraft*, Vol. 22, Sept. 1985, pp. 771-775.

[32]Champange, F. H. and Sleicher, C. A., "Turbulence Measurements with Inclined Hot-Wires, Part 2. Hot-Wire Response Equations," *Journal of Fluid Mechanics*, Vol. 28, Pt. 1, 1967, pp. 177-182.